



Suberoylanilide hydroxamic acid limits migration and invasion of glioma cells in two and three dimensional culture

Zhihua An¹, Christian B. Gluck, Megan L. Choy, Laura J. Kaufman*

Department of Chemistry, Columbia University, New York, NY 10027, United States

ARTICLE INFO

Article history:

Received 16 August 2009

Received in revised form 22 November 2009

Accepted 9 December 2009

Keywords:

Histone deacetylase inhibitor

Glioma

Invasion

Extracellular matrix

ABSTRACT

High grade gliomas are aggressive cancers that are not well addressed by current chemotherapies, in large measure because these drugs do not curtail the diffuse invasion of glioma cells into brain tissue surrounding the tumor. Here, we investigate the effects of suberoylanilide hydroxamic acid (SAHA) on glioma cells in 2D and 3D in vitro assays, as SAHA has previously been shown to significantly increase apoptosis, decrease proliferation, and interfere with migration in other cell lines. We find that SAHA has significant independent effects on proliferation, migration, and invasion. These effects are seen in both 2D and 3D culture. In 3D culture, with glioma spheroids embedded in collagen I matrices, SAHA independently limits both glioma invasion and the reorganization of the tumor surroundings that usually proceeds such invasion. The decreased matrix reorganization and invasion is not accompanied by decreased production or activity of matrix-metalloproteases but instead may be related to increased cell–cell adhesion.

© 2009 Elsevier Ireland Ltd. All rights reserved.

1. Introduction

High grade gliomas are devastating brain tumors that are nearly uniformly fatal despite decades of intensive pre-clinical and clinical research. Although gliomas rarely metastasize outside of the central nervous system, their ability to spread within the brain limits the efficacy of all current treatment strategies [1–8]. Developing effective anti-invasive therapies to be used in combination with other surgical, chemotherapeutic, and radiative approaches is necessary to significantly change the prognosis of patients with these cancers. As a result, many studies have focused on identifying and targeting the cellular mechanisms that underlie glioma invasiveness. Matrix metalloproteases (MMPs), which degrade extracellular matrix components, have long been considered critical ele-

ments in tumor invasion and metastasis. In particular, studies have demonstrated increased expression of the gelatinases MMP-2 and MMP-9 and the membrane-anchored MMP-14 (or MT1-MMP) in and around high grade gliomas [9–16]. While such studies suggest MMP inhibition may be a critical tool in limiting glioma invasion, results of clinical trials of synthetic metalloprotease inhibitors thus far have been disappointing, and the search for effective anti-invasive treatments for high grade gliomas continues [17].

Recently, suberoylanilide hydroxamic acid (SAHA or vorinostat), a histone deacetylase inhibitor (HDACi), has been identified as a very promising anti-cancer drug for its ability to arrest cell growth and induce apoptosis of cancer cells while sparing normal cells in a variety of cell lines [18,19]. SAHA has been the focus of several studies against glioma in particular [20–24]. Administration of SAHA to mouse, rat, and human glioma cell lines in vitro limited cell proliferation and up-regulated pro-apoptotic and anti-proliferative genes including $p^{21/WAF}$ and $p^{27/KIP1}$ [20,22]. In mouse models, SAHA was shown to cross the blood–brain barrier, limit tumor volumetric growth, and increase survival time [20–22].

* Corresponding author. Address: Chemistry Department, Columbia University, 3000 Broadway, Mail Code 3128, New York, NY 10027, United States. Tel.: +1 212 854 9025; fax: +1 212 854 1289.

E-mail address: kaufman@chem.columbia.edu (L.J. Kaufman).

¹ Present address: Department of Chemistry, New York University, New York, NY 10003, United States.

While studies of the effects of SAHA on gliomas thus far have focused on SAHA's ability to halt cell growth and induce apoptosis, other studies suggest SAHA may be an effective anti-invasive compound as well. SAHA decreased tumor necrosis factor driven invasion through Matrigel coated Transwell filters in lung adenocarcinoma cells [25]. Other HDAC inhibitors have also been shown to limit invasion. Trichostatin A (TSA) and tubacin limited transformed fibroblast cell invasion through coated Transwell filters [26,27]. TSA also up-regulated RECK, a membrane glycoprotein that inhibits MMP-2 activity, and limited lung cancer cell invasion through coated filters [28]. Metacept-1 limited MMP-2 expression in treated leukemia cells [29]. Such anti-invasive activity could emerge through an epigenetic mechanism, but it could also arise via direct effects on proteins generally deemed necessary for invasion. Indeed, the structure of SAHA bound to an HDAC-like protein shows the hydroxamic acid group doubly coordinated to a zinc atom [30]. Several broad spectrum MMP inhibitors inhibit MMP activity in exactly the same manner, through binding MMPs via coordination to a zinc atom through a hydroxamate group [31].

While anti-invasive effects of HDAC inhibitors in a number of cell lines has been established, findings on these drugs' effects on cell motility (across uncoated substrates or through uncoated Transwell filters) are less consistent. TSA and SAHA were found to stimulate migration in Ishikawa cells [32]. TSA up-regulated integrins important in migration in hepatocellular carcinoma cells [33], and butyrate promoted migration in colon cancer cell lines [34]. On the other hand, TSA was found to have no effect on the motility of untransformed fibroblasts at concentrations at which invasion was strongly inhibited [26]. TSA has also been found to limit migration of hepatic stellate cells [35].

Given that motility and invasion are both essential in glioma's aggressive dispersion in brain tissue, we have investigated SAHA's effects on several rat and human glioma cell lines in 2D and 3D migration and invasion assays *in vitro*. The 2D assays employed allow independent interrogation of proliferation, migration, and invasion. The 3D assays allow interrogation of proliferation and invasion in an environment in which topology as well as cell–cell and cell–extracellular matrix contacts are similar to those *in vivo*. Such 3D studies are particularly important for study of HDAC inhibitors, as they regulate gene expression, and it is known that both gene expression and cell behavior can be starkly different for cells plated on 2D substrates vs. in 3D environments [36]. In particular, we focus on invasion assays in which glioma cells move through collagen I coated substrates or collagen I gels. We use collagen I as the structural protein in the invasion assays in part because collagen has been shown to be present at substantial levels in and around gliomas [37,38]. Additionally, one of the two primary modes of glioma invasion is along blood vessels, which are rich in collagen I and IV, two of the chief substrates of MMP-2 and MMP-9 [1,5]. Finally, gliomas invade very aggressively in collagen I gels *in vitro*, and such gels are increasingly being used as 3D environments in which to study glioma invasion [39–43].

In the 2D and 3D assays performed, we find that SAHA strongly inhibits cell proliferation but does not substantially

induce cell death at concentrations up to 5.0 μM . Migration and invasion assays show that SAHA inhibits rat C6 and human U87 migration and invasion at ≤ 10.0 and 5.0 μM , respectively, when plated on 2D substrates. For multicellular tumor spheroids of 5 different glioma cell lines embedded in 3D collagen I matrices, SAHA strongly inhibits invasion at concentrations ≥ 2.5 μM . We also find that SAHA independently affects cell reorganization of the tumor surroundings and invasion into those remodeled surroundings. Preliminary investigation into the mechanisms by which SAHA limits glioma invasion shows that SAHA does not strongly bind secreted MMP-2 or MMP-9, despite the similarity in structure between SAHA and some MMP inhibitors. Moreover, zymography shows that MMP-9 is up-regulated in the presence of SAHA. This is consistent with quantitative real-time PCR analysis; however, such analysis also shows other proteases are down-regulated, and other genes important in cell–matrix interactions are affected. We suggest that increased cell–cell adhesion in the presence of SAHA may be the most important factor in SAHA's ability to limit invasion of glioma cells cultured in a 3D environment.

2. Materials and methods

2.1. Cells

WI-38 and 3T3 fibroblasts and LN18, F98, and F98EGFR-vIII glioma cells were purchased from the American Type Culture Collection and cultured in medium per the supplier's instructions. C6 and U87 glioma cells were provided by Prof. Peter Canoll at Columbia University Medical School and cultured in DMEM supplemented with 10% fetal bovine serum (FBS), 100 U/ml penicillin, 100 $\mu\text{g}/\text{ml}$ streptomycin, and 0.25 $\mu\text{g}/\text{ml}$ amphotericin B.

2.2. Drugs and chemicals

SAHA was provided by Prof. Ronald Breslow and diluted in DMSO. In all studies, an equivalent amount of DMSO without SAHA was added to the control culture medium. Dulbecco's modified eagle media (DMEM), Dulbecco's phosphate buffered saline (D-PBS), trypsin–ethylenediaminetetraacetic acid (trypsin–EDTA), FBS, calf serum, an antibiotic–antimycotic [containing penicillin, streptomycin, and amphotericin], and 4',6-diamidino-2-phenylindole (DAPI) were purchased from Invitrogen. A live/dead cell staining kit (L3224) used in 2D proliferation and viability assays and a CyQuant kit used in 3D proliferation and viability assays (7026) were also purchased from Invitrogen. Trypan blue solution (0.4%) was purchased from Sigma–Aldrich. Pepsin-solubilized type I collagen was purchased from Inamed Biomaterials. Collagenase type I (4000 U/mL) was purchased from Invitrogen (17100). Zymograph gels, buffers, Coomassie Blue R-250 Staining Solutions kit and SDS–PAGE standards were obtained from BioRad.

2.3. 2D proliferation and viability assay

A dye exclusion method was used to measure cell viability and proliferation. 5×10^4 cells were seeded in

1.0 ml of medium in 24-well plates, with biological triplicates performed for all SAHA concentrations. SAHA was added in the concentrations indicated 24 h after seeding and cultured for the times indicated. Cells were collected after trypsinization and washed with PBS buffer. 100 μ l cell suspension was mixed with 100 μ l 0.4% trypan blue, which is excluded by live cells but stains dead cells. The cell solution was allowed to stand for 5 min at room temperature. A cytometer was used to count total number of cells and dead (stained) cells. Viable cell percent was calculated relative to control (untreated) samples. Each data point was obtained from the average of triplicate cell culture. The same method was used to measure proliferation and viability of cells plated on collagen coated substrates in the absence and presence of SAHA. Here, each well of 24-well plates was coated with 1.0 ml of 0.1 mg/ml collagen I solution at 37 °C. After 2 h, 1×10^5 cells were seeded on the collagen coated plates and incubated overnight. Medium containing SAHA was added, and cells were incubated for 24 h. Collagen was dissolved with a 1.0 mg/ml collagenase I solution for 30 min, and cells were collected. The remaining steps were identical to those described above.

2.4. Transwell migration and invasion assays

Transwell chambers with polycarbonate membranes and 8 μ m pores were used for migration and invasion assays. The migration (invasion) assays were done through uncoated (collagen I coated) Transwell filters. For the invasion assays, 300 μ l of 0.1 mg/ml collagen I solution was placed in the top compartment and incubated at 37 °C for 2 h. For both migration and invasion assays, 1.0 ml of cells at 1×10^5 cells/ml was seeded on the uncoated or coated membrane overnight, 300 μ l serum free medium with SAHA in a concentration series was added to the upper chamber and 500 μ l medium with serum was added to the lower chamber. Cells were allowed to invade for 24 h. Non-invasive cells were then removed from the upper chamber, and the invasive cells present on the underside of the membrane were fixed and stained with DAPI. Automated counting of cells was performed using a program written for this purpose. The number of invasive cells was computed per field for five fields selected at random on each membrane. Experiments were done in triplicate.

2.5. Preparation of multicellular tumor spheroids and collagen gels

Glioma cells were cultured in DMEM supplemented with 10% FBS, 100 U/ml penicillin, 100 μ g/ml streptomycin, and 0.25 μ g/ml amphotericin B. Multicellular tumor spheroids (MTSs) of uniform size and shape were formed using a hanging drop procedure. 20 μ l (~200 cells) of cell solution was dropped onto the inside cover of a 100 mm Petri dish, and the Petri dish was filled with 10 ml culture medium. The dish was inverted and incubated for 7 days. The drops were held in place by surface tension, and the cells accumulated at the bottom of the droplet to form the spheroids. Collagen solutions were prepared from a stock collagen I solution at 3.1 mg/ml, 10 \times DMEM solution, 7.5% w/w sodium bicarbonate, pre-prepared culture

medium for cell culture, and NaOH (0.1 N). Sodium bicarbonate (7.5% w/w) in a volume equal to 2% of the total volume of the gel was added. NaOH was added to bring the pH to 7.4, and culture medium was added to ensure cell health during the experiment. The solution was well mixed and kept at 4 °C before placement into homemade sample cells. The sample cells consist of 2 cm diameter plexiglass cylinders of height up to 2 cm and are fully sealed with UV epoxy on glass coverslips. Nylon mesh was placed around the circumference of the cylinders to allow the collagen gels to anchor and prevent collapse of the gels under tension from migrating cells. A single spheroid of ~400 μ m in diameter was collected and deposited into 600 μ l 1.0 mg/ml collagen (with desired concentration of SAHA) solution. Sample cells were covered and incubated at 37 °C and 5% CO₂. Full gelation occurred within one hour, and a superlayer of culture medium with the same concentration of SAHA as that in the gel was then added to maintain moisture and pH. In all assays except those specified, SAHA treatment of spheroids began when the spheroid was deposited into the SAHA containing collagen solution. For interrogation of whether SAHA can affect early invasive behaviors, some MTSs were pre-treated with SAHA before being placed in collagen gel. In these cases, developing spheroids were incubated in the hanging drop with the desired concentration of SAHA for 24 h before implantation. The remaining steps were identical to those described above.

2.6. 3D proliferation and viability assays

To measure the viability and proliferation of the MTSs, a modified CyQuant assay was performed on spheroids cultured in the presence or absence of SAHA for up to 3 days. Collagen gels containing MTSs were degraded via treatment with collagenase I solution for one hour at 37 °C. After centrifugation, treatment of the cell pellet with a 0.5% solution of trypsin-EDTA was performed until the pellet was broken up as judged by visual inspection. The resulting cell suspension was centrifuged and washed twice with PBS. After centrifugation, the cell pellet was resuspended in 200 μ l 2 \times CyQuant-GR dye solution and aliquoted to a 96 well plate. The plate was incubated at 37 °C for 10 min and then placed in a plate-reading spectrophotometer with excitation at 480 nm and detection at 520 nm. Measured fluorescence represents the number of dead cells in the sample. Following this, 20 μ l of 20 \times lysis buffer was added to each well, and the plate was stored at -80 °C for 20 min. After allowing the plate to thaw to room temperature, it was incubated at 37 °C for an additional 20 min. The plate was again read at 480/520 nm. The fluorescence intensity represents the total number of cells per sample. All fluorescence measurements were compared to a standard curve, which correlated fluorescence intensity with cell number. Three MTSs were measured in each case. Live/dead cell staining was also used to ascertain the location of dead cells in the MTSs. Tumor spheroids were cultured in collagen I gel with SAHA for three days, the gels with spheroids were washed with PBS buffer three times, and 1.0 ml live/dead stain solution comprised of 2.0 μ M Calcein AM and 4.0 μ M EthD-1 was

added to the cylinder for 30 min at room temperature. Images were then taken as described in Section 2.8.

2.7. 3D invasion assay

Spheroids embedded in collagen gels were removed from the incubator and imaged with bright field microscopy at 2, 5, 9, 24, 48, and 72 h after implantation. Spheroid radius and invasive distance (as illustrated in Fig. 3) were recorded for six spheroids at each SAHA concentration for C6 cells and two spheroids at each concentration for all other cell lines.

2.8. Optical microscopy

Transmitted light images were taken on an Olympus Fluoview 300/IX-71 in scanning mode using an Argon ion laser at 488 nm for excitation and a photomultiplier tube (PMT) for detection. Confocal fluorescence microscopy (CFM) with excitation via either an Argon ion laser at 488 nm or a Helium Neon laser at 543 nm, a 60× oil objective, and appropriate filter sets dichroics and bandpass filters was used to image the spheroids after live/dead staining. To image the collagen matrix, confocal reflectance microscopy (CRM) was employed, and 488 nm light that leaked through the dichroic mirror was collected on the PMT.

2.9. Gelatin zymography

An equal number of C6 glioma cells were cultured with and without SAHA for 24 h. Protein was collected from the culture medium and concentrated using ultracentrifugation. Total protein concentration was determined by the Bradford assay. 25 µg total protein was size separated on 10% SDS-PAGE gels containing gelatin at a final concentration of 1.0 mg/ml. Gels were incubated with renaturation buffer (2.5% Triton) for 30 min and development buffer (pH 8.0 Tris buffer containing 5 mM calcium chloride) overnight and then were stained with Coomassie Blue for 30 min. Clear bands show gelatinase activity after destaining the gel for more than 2 h.

2.10. Quantitative real-time PCR analysis

For PCR analysis, cells were cultured in the absence and presence of 5.0 µM SAHA. 10⁶ cells were suspended in 10 ml culture medium with 0.1 mg/ml collagen I and 20 µl SAHA stock solution in DMSO in a culture dish. An equal amount of DMSO was added to the control sample. After culture for 24 h at 37 °C, 10 ml 1.0 mg/ml collagenase I in PBS solution was added and incubated for 1 h. Centrifugation was performed, cells were collected and washed with PBS, and cells were snap frozen as pellets in liquid nitrogen for 2 min and stored at –80 °C until sent for PCR analysis. RNA was extracted and amplified, and PCR analysis was performed by SABiosciences Corporation in duplicate. An 84 gene array focusing on ECM and adhesion molecules (RT² Profiler™ Array: PARN-013) was used [44]. Measurements of mRNA for these 84 genes were reported via the SYBR Green PCR detection method. The data was normalized to 5 housekeeping genes and quantitation

was performed via the comparative C_t method. Genes that were up- or down-regulated by at least 2-fold compared to the control with *p* < 0.01 after a *t*-test are reported.

2.11. Adhesion assay

A procedure based on spheroid preparation and inspired by a qualitative adhesion assay described in Ref. [39] was used to interrogate changes in cell–cell adhesion under SAHA treatment as follows: 20 µl (~200 cells) of cell solution without or with SAHA was dropped onto the inside cover of a 100 mm Petri dish that was then filled with 10 ml culture medium. The dish was inverted and incubated for 40 h. The drops were held in place by surface tension, and the cells accumulated at the bottom of the droplet to form clusters. The Petri dishes were transferred to the microscope where cell aggregates were observed via bright field microscopy. Between 2 and 5 aggregates were assessed in this manner at each SAHA concentration.

3. Results

3.1. SAHA arrests glioma cell growth

We determined the effect of SAHA on normal human lung fibroblasts (WI-38), NIH fibroblasts (3T3) and rat (C6) and human (U87) glioma cells. SAHA inhibited cell growth of WI-38, 3T3, C6, and U87 cells at concentrations ≥ 1.0 µM (Fig. 1A–C). After 72 h of treatment at 1.0 µM, cell number decreased by 29%, 59%, and 38% for the WI-38, 3T3, and C6 cells, respectively. The differential in arrest of cell growth between untransformed and transformed and cancer cells is consistent with that found previously [45]. Additionally, it appears that C6 and U87 cell proliferation are very similarly affected by SAHA, with cell number decreasing by 85% in U87 cells treated for 72 h at 2.5 µM SAHA compared to 89% for C6 cells. This result is similar to that measured previously [20]. While SAHA effectively inhibited the growth of the transformed and glioma cells investigated at concentrations similar to those found effective previously, SAHA did not induce cell death at these concentrations (Fig. 1E,F). Indeed, at concentrations up to 5.0 µM, we find no decrease in cell viability relative to control at 72 h of culture. This effect has also been seen previously for U87 cells, though increasing cell death was seen in this case for treatment of 5–7 days [22].

3.2. Two dimensional assays: SAHA inhibits glioma cell migration and invasion

The effect of SAHA on glioma cell migration and invasion was studied by Transwell assays described in Section 2.4. The migration assays were performed by allowing treated cells to move through uncoated Transwell filters with pores of 8 µm. As shown in Fig. 2A (cross-hatched bars), the number of C6 cells that migrate through the uncoated filters decreases with increasing SAHA concentration. To ascertain whether the decrease in migrating cells is due to a decrease in viable cell number or a decrease in migratory capacity, we calculate number of cells expected to cross the filter given no effect of SAHA on migratory capacity as follows:

$$\text{Cells}_{\text{mig.exp}}(\text{xM}) = \text{Cells}_{\text{mig.obs}}(\text{0M}) \\ * \text{Cell Number Ratio} * \text{Cell Viability Ratio}, \quad (1)$$

where Cells_{mig.obs}(0 M) is the number of cells that migrate through the filter in the absence of SAHA. Cell Number Ratio is the total number of cells after 24 h of culture at a given SAHA concentration divided by that in the absence of SAHA. Cell Viability Ratio is the percent viable cells at a given SAHA concentration divided by that in the absence of SAHA. Data used to determine Cell Number Ratio and Cell Viability Ratio for C6 cells is shown in Fig. 1C and F. Expected (light bars) vs. observed (dark bars) number of cells that migrate through the filter as a function of SAHA concentration is plotted in Fig. 2B. This confirms that SAHA affects migration of C6 cells through uncoated Transwell filters at concentrations of 10.0 and

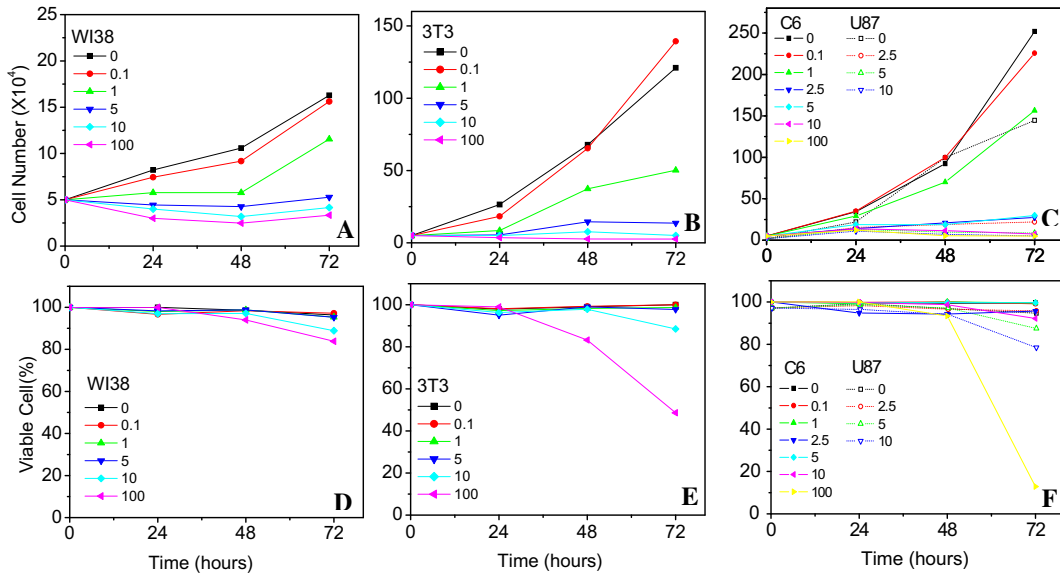


Fig. 1. The effect of SAHA on cell growth and viability of normal fibroblasts (WI-38, A and D), transformed fibroblasts (3T3, B and E) and glioma tumor cells (C6 and U87, C and F) in culture. The cells were cultured without or with SAHA in the concentrations indicated for up to 72 h.

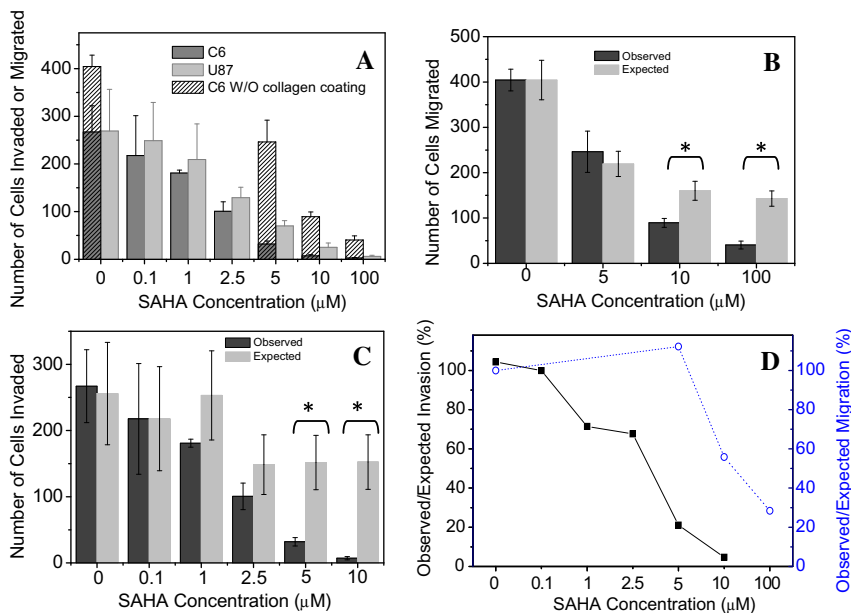


Fig. 2. The effect of SAHA on glioma cell invasion through Transwell filters. (A) Number of C6 cells (cross-hatched bars) that migrate through uncoated Transwell filters and number of C6 (dark filled bars) and U87 (light filled bars) cells that invade through collagen I coated Transwell filters over 24 h as a function of SAHA concentration. (B) C6 cells expected (light filled bars) and observed (dark filled bars) to pass through the uncoated Transwell filter as a function of SAHA concentration. (C) C6 cells expected (light filled bars) and observed (dark filled bars) to pass through coated filters as a function of SAHA concentration. (D) Cell migration (right axis) and cell invasion (left axis) changes as captured by ratio of observed to expected cells that invade through uncoated and coated chambers, respectively. In (B) and (C), statistically significant differences between expected and observed data are indicated with an asterisk. In all cases, unpaired two-tailed *t*-tests are performed, and $p \leq 0.01$ are reported as significant.

100 μM, though not at 5.0 μM, as assessed by unpaired two-tailed *t*-tests. We then perform the same assay on both C6 and U87 cells on Transwell chambers coated with collagen I: this assay assesses both migration and invasion. Absolute number of invading U87 and C6 cells is similar

(Fig. 2A). For untreated C6 cells, 34% fewer cells migrate through coated Transwell filters than uncoated ones, showing that the presence of collagen limits the number of cells that invade. The ratio of cell invasion (through coated filters) to cell migration (through uncoated filters) de-

creases at increasing SAHA concentration (66%, 13%, 8%, and 7% at 0, 5.0, 10.0, and 100 μM SAHA, respectively) (Fig. 2A), showing that SAHA has an

independent effect on cell migration and cell invasion. To quantify effects of SAHA on cell invasion, we calculate the number of cells expected to in-

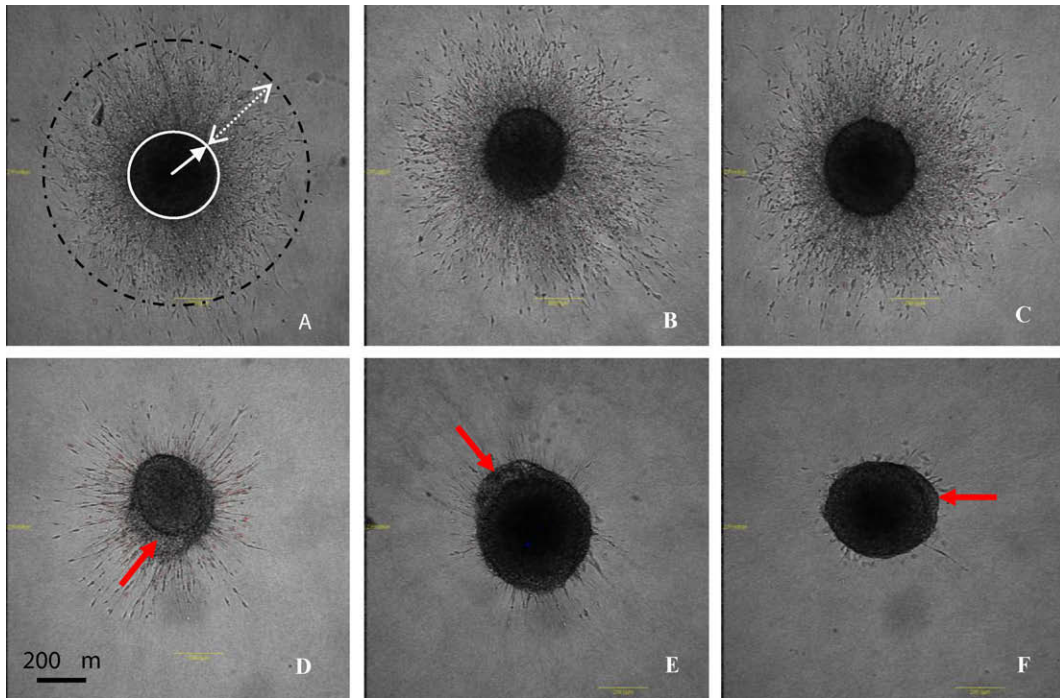


Fig. 3. Bright field images of C6 MTSs in collagen I gels of 1.0 mg/ml. The imaged MTSs were embedded in the collagen gels for 24 h with (A) 0 μM , (B) 0.1 μM , (C) 1.0 μM , (D) 2.5 μM , (E) 5.0 μM and (F) 10.0 μM SAHA. Spheroid radius (solid arrow) and invasive distance (dotted arrow) are depicted on the spheroid in (A). Arrows in (D–F) denote regions of the spheroid that are unusually shaped and less dense than typical.

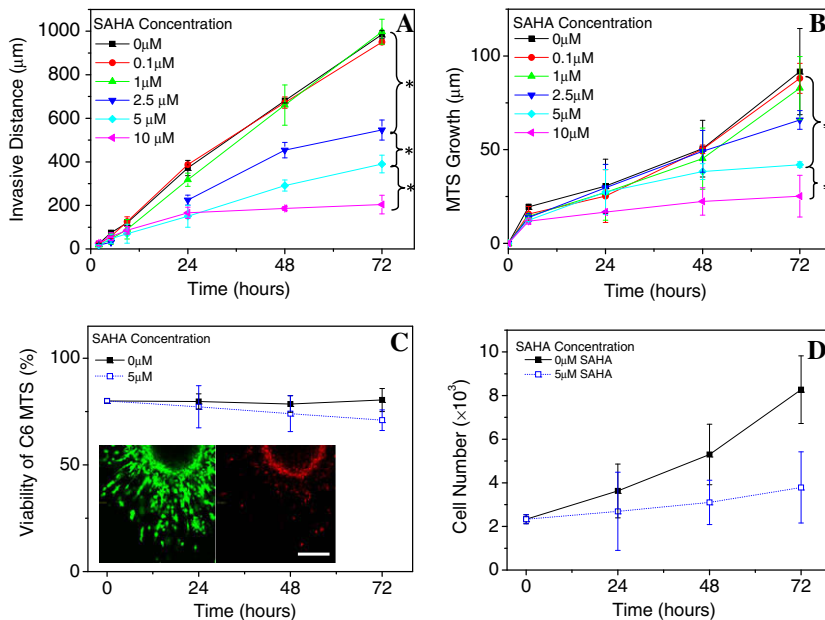


Fig. 4. (A) Invasive distance and (B) spheroid radius growth for C6 as a function of SAHA concentration over 72 h. Statistically significant differences at 72 h are indicated with an asterisk. Statistical relevance is assessed via unpaired two-tailed *t*-tests. In (A), indicated results have $p \leq 0.0001$. In (B), indicated results have $p \leq 0.005$. (C) Viability and (D) proliferation of C6 cells cultured as spheroids in collagen gels in the absence (solid lines) and presence (dashed lines) of 5.0 μM SAHA. Inset of (C): CFM slice of a C6 spheroid treated with 5.0 μM SAHA for 3 days and stained with (left) calcein AM, which stains live cells and (right) EthD, which stains dead cells. Scale bar is 200 μm .

vade through the coated filter taking into account SAHA's effects on cell proliferation and viability:

$$\text{Cells}_{\text{inv.exp}}(xM) = \text{Cells}_{\text{inv.obs}}(OM) \times \text{Cell Number Ratio} \times \text{Cell Viability Ratio}, \quad (2)$$

with Cell Number Ratio and Cell Viability Ratio now obtained from data for cells cultured on collagen I coated surfaces after 24 h of treatment (Supp. Fig. 1). We note that for C6 cells cultured in this way, cell viability is slightly lower but proliferation somewhat less affected by SAHA at 24 h of treatment compared to cells cultured on uncoated surfaces (Supp. Fig. 1 vs. Fig. 1C and F). The ratio of observed to expected number of cells that pass through the coated membrane decreases with increasing SAHA concentration. The decrease in cells that pass through coated filters represents both diminished migration and invasion and becomes statistically relevant at 5.0 μM SAHA (Fig. 2C). Fig. 2D displays the ratio of observed to expected cells that pass through both uncoated (dashed line) and coated (solid line) membranes. The dashed line indicates that C6 migration is affected at SAHA concentrations of 10.0 μM and above. All remaining inhibition seen for the coated Transwell filters represents decrease in invasion due to SAHA. Thus, at concentrations of 1.0 μM and higher, SAHA inhibits invasion through collagen I gels. In sum, our 2D assays show that SAHA independently affects C6 proliferation, migration, and invasion.

3.3. Three dimensional assay: SAHA reduces invasive cell density and speed

To investigate whether SAHA inhibits glioma invasion in an environment in which cell–cell and cell–environment contacts are more similar to those found in vivo, 3D invasive assays were done on glioma cells as

described in Section 2.7. Fig. 3 shows representative bright field images of C6 MTSs in collagen gel matrices without SAHA and with increasing concentrations of SAHA 24 h after implantation. Invasive cells are observed to emerge from the central portion of the MTS, which is densely packed with cells. Several changes are evident with increasing SAHA concentration, with obvious changes at SAHA concentrations at and above 2.5 μM . First, there is decreasing invasive cell density as SAHA concentration increases. Additionally, the distance that invasive cells traverse decreases as a function of increasing SAHA concentration. Finally, the central portion of the spheroid becomes less homogeneous, with less dense areas found at the spheroid rim than is seen for untreated spheroids and spheroids treated at ≤ 1.0 μM SAHA (arrows, Fig. 3).

To quantify the effect of SAHA on the growth and invasion of C6 glioma MTS, invasive distance and spheroid radius as function of SAHA concentration were measured over 72 h (Fig. 4A,B). Each trace in Fig. 4A and B is derived from an average over six MTSs. The invasive distance data shows that cells invade very quickly in environments with SAHA concentrations ≤ 1.0 μM . In contrast, spheroids treated with 2.5–10.0 μM SAHA invade very slowly, and this effect is most obvious after 72 h of invasion. Unlike in the 2D assays, there is no obvious way to distinguish inhibition of proliferation, migration, and invasion in this 3D assay. However, it is clear that SAHA affects invasion in 2D in a statistically relevant manner at 5.0 μM concentration and affects a combination of proliferation, migration, and invasion in this 3D assay (as probed by invasive distance and spheroid radius) at even lower concentrations. While invasive cell density is difficult to quantify [46], visual observation shows that the number of invasive cells is vastly decreased at these SAHA concentrations as well (Fig. 3). To ascertain whether the decreases in invasive cell density and distance are related to decrease of cell proliferation and/or viability in the spheroid in the presence

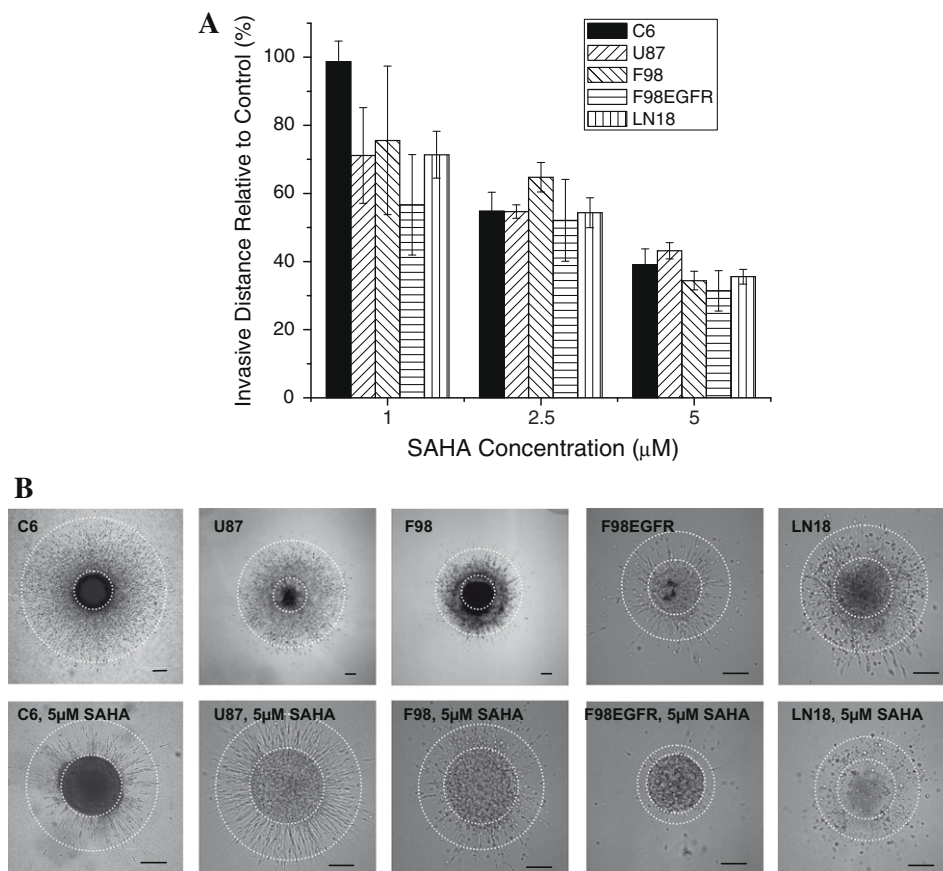


Fig. 5. (A) Invasive distance relative to control for 5 glioma cell lines cultured in spheroid with 1.0, 2.5, and 5.0 μM SAHA for 72 h. (B) Representative images for all cell lines of untreated spheroids 72 h after implantation and spheroids treated at 5.0 μM 72 h post-implantation. Central portion of spheroid and average extent of invasive cells from which spheroid radii and invasive distances are calculated are shown for each depicted spheroid. Scale bar is 200 μm in all cases.

of SAHA, live and dead cell number were measured in spheroids over 72 h for untreated spheroids and those treated with 5.0 μM SAHA. Over 72 h of treatment, we find cell viability similar in the control and 5.0 μM treated spheroids (Fig. 4C). Cell proliferation is affected, but somewhat less than for cells cultured on 2D, where proliferation is inhibited by $\sim 90\%$ by 72 h of treatment at 5.0 μM (Fig. 1C). In spheroid culture, proliferation is inhibited by $\sim 45\%$ by 72 h of treatment at 5.0 μM (Fig. 4D). To confirm the cell viability measurements as performed with the CyQuant assay and to visualize the areas of the spheroid that contain dead cells, we performed Calcein AM and EthD-1 staining to label live and dead cells, respectively. CFM images show that after treatment with SAHA for 3 days, in all spheroids there are some dead cells in the center of the spheroid (*data not shown*). Taking a slice near the middle of the spheroid for cells cultured with 5.0 μM SAHA for 72 h reveals a substantial number of dead cells in the spheroid rim where proliferative cells normally exist (Fig. 4C, inset). However, many live cells also exist in the proliferative rim and if SAHA affected only cell viability and proliferation, we would expect a substantial number of those cells to invade the surroundings.

To determine whether the substantial inhibition of invasiveness seen in C6 cells treated with SAHA is present in other glioma cell lines, including those with mutations often seen human glioblastomas, spheroid growth and invasion was also measured for U87, F98, and F98EGFRvIII, and LN18 cells. Invasive distance is plotted over 72 h at SAHA concentrations from 1.0–10.0 μM (Supp. Fig. 2). Inhibition of invasive distance relative to untreated spheroids of the same cell line for SAHA treatment at 1.0, 2.5, and 5.0 μM after 72 h is shown in Fig. 5, as are representative images for untreated spheroids and spheroids treated at 5.0 μM after 72 h. For all cell lines, invasive distance is similarly affected, with at least 50% invasive distance inhibition at 72 h at 5.0 μM SAHA. Images in Fig. 5 also clearly show that all cell lines cultured in spheroid show substantial decrease in invasive cell density with SAHA treatment. We also note that the various cell lines show somewhat different patterns of invasion in the collagen I gels [39]: C6 and U87 cells show a dispersed pattern of invasion, F98 cells show a ring pattern, F98EGFRvIII cells show a compact pattern, and LN18 cells show an unusual pattern similar to the compact pattern. After SAHA treatment, C6, U87, F98, and F98EGFRvIII spheroids all have compact patterns of invasion, with few invasive cells that are almost all within two cell lengths of the dense portion of the spheroid body. LN18 spheroids are an exception and appear to have very unorganized spheroids and invasion patterns after SAHA treatment. While invasive distance inhibition, invasive cell density, and invasion patterns are altered similarly in all cell lines (except LN18), MTS growth inhibition upon SAHA treatment varies somewhat more (*data not shown*). C6, U87, and LN18 cells all show similar MTS growth inhibition with SAHA treatment (46%, 36%, and 53%, respectively, at 72 h at 5.0 μM SAHA), but F98EGFRvIII cells show similar MTS growth in the presence and absence of SAHA and F98 cells show somewhat increased MTS growth in the presence of SAHA, which is potentially related to the transition from the ring-like to compact invasion pattern.

3.4. Three dimensional assay: SAHA inhibits glioma ability to reorganize the surroundings

The transition to the compact invasive pattern and significantly decreased invasive cell density after SAHA treatment suggests that SAHA may be altering the relative preference of glioma cell–cell and cell–environment interactions. To further interrogate why few live cells leave the proliferative rim and invade the surrounding gel, we also image the collagen surrounding the spheroids as they invade. Fig. 6 shows confocal reflectance images (CRM) of C6 MTSs and surrounding collagen fibers (left panel) and bright field images of the MTSs (right panel) 24 h after implantation. Collagen fibers appear aligned in a starburst pattern around untreated spheroids. Invasive cells preferentially move along paths set up by the initial invasive cells that reorganize these collagen fibers and invade along them, as has been described previously [40]. Aligned fibers are also present around spheroids treated with 5.0 μM SAHA (Fig. 6B). This suggests that SAHA treatment upon implantation (post-treatment) does not prevent the earliest activity of invasive cells, the generation of traction on the collagen fibers that results in their organization into the starburst pattern. It does show, however, that cell driven alignment of the matrix is not a sufficient condition to allow for cells to invade into these surroundings. To further assess how SAHA affects cell interaction with collagen in these gels, we embedded C6 MTSs pre-treated with 5.0 μM SAHA as described in Section 2.5. In this case, very little alignment

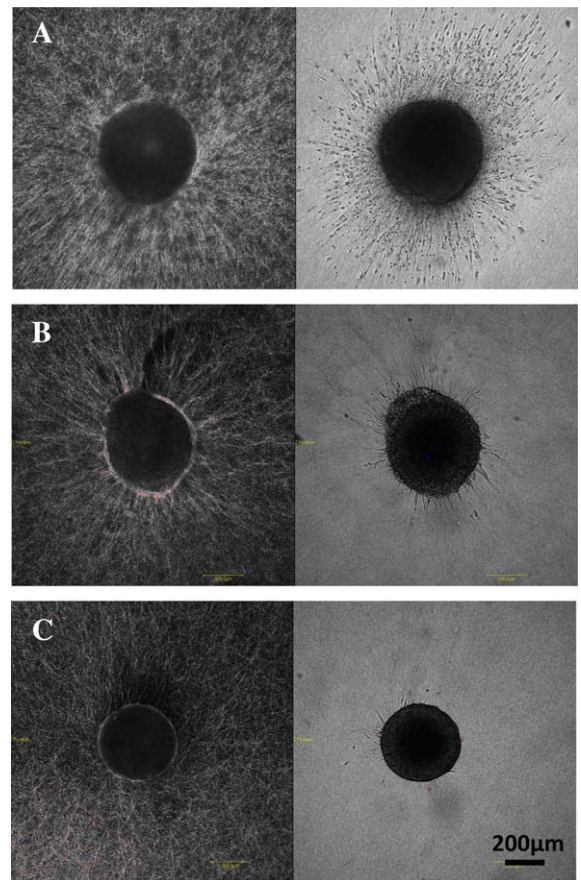


Fig. 6. CRM images of spheroids and surrounding collagen fibers (left panel) and bright field images of spheroids (right panel) collected simultaneously 24 h after implantation. (A) Untreated spheroid. (B) Spheroid treated with 5.0 μM SAHA. Treatment began upon implantation and is termed post-treatment in the text. (C) Spheroid pre-treated with 5.0 μM SAHA.

of the collagen is apparent and even fewer invasive cells are present than for the spheroid treated upon implantation (Fig. 6B and C). This finding suggests that there is an induction time before SAHA inhibits the ability of cells to align the matrix. Moreover, the differential in invasive cells in the pre-treated, post-treated, and untreated cells suggests that in 3D collagen I culture, SAHA independently inhibits remodeling of collagen I surroundings and invasion into these (aligned or not) surroundings. We can not distinguish whether more cells invade in post-treated than in pre-treated spheroids due to the presence of the aligned matrix in the former or because there is an induction time before which SAHA does not affect invasion.

3.5. Zymography

The fact that C6 invasion in spheroid is strongly inhibited even when the cells can reorganize matrix suggests that the inhibition of invasion persists even in ideally remodeled environments. In such environments, invasion inhibition may emerge from a variety of sources including inability for cells to detach from the spheroid and lack of activity of proteases that dissolve extracellular matrix structures and make the matrix (even once aligned) more permissive of invasion. Given SAHA's structural similarity to some MMP inhibitors, the fact that C6 spheroids treated with the broad spectrum MMP inhibitor GM6001 look similar to those treated with SAHA (*data not shown*), and the accumulated evidence suggesting MMPs are important in glioma invasion in vivo [9–16], we investigated

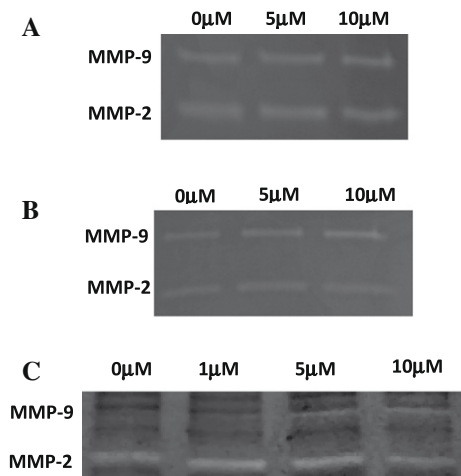


Fig. 7. Gelatin zymography of MMP-2 and MMP-9. The bands indicate MMP-2 and MMP-9 activity. (A) MMPs collected from culture medium of untreated glioma cells, mixed with SAHA, and incubated for 24 h prior to zymography, (B) MMPs collected from the culture medium of the same number of C6 cells cultured with SAHA for 6 h. (C) MMPs collected from the culture medium of the same number of C6 cells cultured with SAHA for 24 h.

SAHA's effects on MMP activity and production. To assess whether the presence of SAHA can affect gelatinase (MMP-2 and MMP-9) activity by direct binding to these MMPs produced by the glioma cells, we collected culture medium from untreated C6 cells cultured for 24 h on an uncoated culture dish and mixed this cell-conditioned medium with SAHA for 24 h before performing zymography. Fig. 7A shows that clear bands were found for both MMP-2 and MMP-9 regardless of SAHA concentration, indicating that SAHA does not strongly bind MMP-2 or MMP-9, consistent with activity-based profiling that showed SAHA to be quite selective for HDACs [47]. To explore whether SAHA affects the production of either of these gelatinases, we measured the amount of MMP-2 and MMP-9 in the medium of SAHA treated cells through zymography after 6 and 24 h of treatment (Fig. 7B and C). At both 6 and 24 h, a modest increase in MMP-9 activity is seen at 10.0 μM SAHA, while at 6 h no change in MMP-2 is found and at 24 h, a modest decrease is evident for SAHA concentrations greater than 5.0 μM .

3.6. Three dimensional assay: SAHA alters glioma cell–cell adhesion

Given that zymography showed no clear decrease in MMP-2 or MMP-9 activity, and even showed increased MMP-9 production, decrease in gelatinase activity does not appear to be the cause of the decreased spher-

oid invasion seen upon SAHA treatment. Another possible origin of decreased invasion, both in spheroid in vitro and in tumors in vivo, is increased glioma cell–glioma cell adhesion. Increased cell–cell adhesion upon SAHA treatment could indeed lead to the changes from dispersed or ring-like invasion to a compact invasion pattern. Indeed, the dispersed and ring invasion pattern in collagen I gels have been shown to correlate with low to moderate N-cadherin levels in glioma cells, while the compact invasive pattern correlates with low levels of MMP gene expression and high N-cadherin levels [39]. To further test the hypothesis that increased cell–cell adhesivity occurs with SAHA treatment, a qualitative adhesion assay was developed. Cells were plated as usual for the preparation of spheroids. For C6 cells under these conditions, formation of relatively tight spheroids of uniform size and spherical shape typically takes 7 days. Here, we imaged cells in the hanging drop with or without SAHA treatment after 40 h. Fig. 8 shows typical C6 aggregates after 40 h in the hanging drop with no treatment and upon treatment with 5.0 μM SAHA. It is apparent that cells form more adherent aggregates in the presence of SAHA. Indeed, as a function of SAHA concentration, a monotonic decrease in the average number of aggregates and an increase in the smoothness of the aggregate surface (*data not shown*) is seen.

3.7. Quantitative real-time PCR

The results of zymography and the cell adhesion study suggest it is more likely the decreased invasiveness of C6 cells in vitro in the presence of SAHA is due to increased cell–cell adhesion than to decreased matrix degradation. To more broadly assess the mechanism through which SAHA may affect C6 invasion, we performed real-time PCR on C6 cells cultured in 3D collagen gels to search for invasion-related genes up-regulated or down-regulated by SAHA for cells cultured in 3D environs. A PCR array from SABiosciences with 84 genes important in cell–cell and cell–matrix interactions was used. The genes included in the array can be found in Ref. [44]. The array was performed on control cells and C6 cells cultured in 3D collagen I gels and treated with SAHA at 5.0 μM for 24 h. MMP-2 was down-regulated 1.92-fold and MMP-9 was up-regulated 4.57-fold, consistent with zymography (Fig. 7). However, *t*-tests revealed these measurements to not be statistically significant (*p*-values of 0.095 and 0.015, respectively). Of the genes that were up-regulated or down-regulated at least twofold, 14 had a *p*-value of <0.01. These genes (as well as MMP-2 and MMP-9) are shown in Table 1. The expression of a variety of collagens and other ECM molecules are altered by SAHA, though as many are up-regulated as down-regulated. Of the 21 proteases and protease inhibitors interrogated, only the gene predicted to correlate with MMP-15 was significantly affected. Of the 3 tissue inhibitors of MMPs assessed, 1 was down-regulated, 1 was slightly up-regulated, and 1 was up-regulated more substantially (TIMP-1 was up-regulated 3.64-fold, *p* = 0.01). Of the 9 cadherins or cell–adhesion molecules measured, 7 were up-regulated. Among these are N-cadherin (up-regulated 1.39-fold, *p* = 0.06) and E-cadherin (up-regulated 8.64-fold, *p* = 0.07). However, of these 9 genes, only one was altered in a statistically relevant manner: platelet endothelial cell adhesion molecule (PECAM, CD31) was strongly

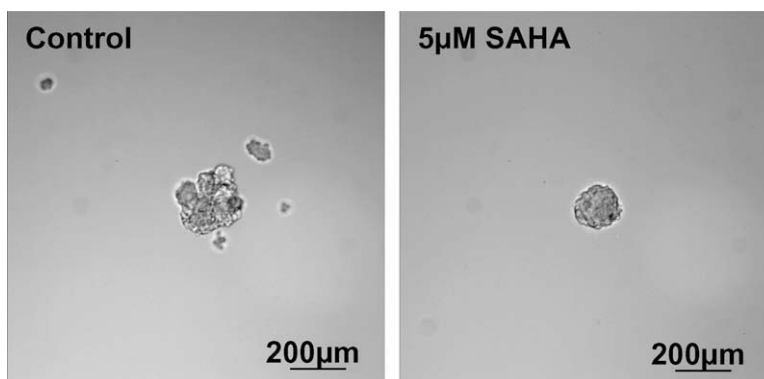


Fig. 8. Representative images of C6 cell aggregates that develop in a cell adhesion assay described in Section 2.11. (Left) Untreated sample has a large apherical aggregate and several satellite aggregates. (Right) Cells treated with 5.0 μM SAHA are tightly packed into a single, spherical aggregate.

Table 1RT-PCR results for C6 cells cultured in 3D in collagen I gel in the absence and presence of 5.0 μ M SAHA.

Gene	Category of function	Up- or down-regulation	p-value
Procollagen, type II, alpha 1	ECM structural constituent	−3.93	0.0034
Procollagen, type III, alpha 1	ECM structural constituent	−6.27	0.0022
Procollagen, type IV, alpha 3	ECM structural constituent, ECM protease inhibitor	3.06	0.0062
Chondroitin sulfate proteoglycan 2	ECM molecule	−5.14	0.0028
Extracellular matrix protein 1	ECM molecule	9.64	0.0032
Ectonucleoside triphosphate diphosphohydrolase 1	Extracellular mediator	36.71	0.0032
Integrin beta 4	Cell matrix adhesion transmembrane molecule,	21.63	0.0026
Laminin, alpha 1	Adhesion molecule	5.61	0.0073
Matrix Metalloprotease 15	ECM protease, transmembrane molecule	−8.78	0.0063
Platelet/endothelial cell adhesion molecule	Transmembrane molecule	31.06	0.0048
Selectin, lymphocyte	Transmembrane molecule	7.04	0.0018
Sarcoglycan, epsilon	Transmembrane molecule	−2.19	0.0009
Synaptotagmin I	Transmembrane molecule	11.21	0.0068
Thrombospondin 2	Adhesion molecule	2.47	0.0046
Matrix metalloprotease 2	ECM protease	−1.92	0.095
Matrix metalloprotease 9	ECM protease	4.57	0.015

up-regulated (up-regulated 31.06-fold, $p = 0.005$). The two other genes that RT-PCR showed to be most substantially affected are integrin β_4 and ectonucleoside triphosphate diphosphohydrolase 1 (ENTPD1).

4. Discussion

The poor prognosis of patients with glioblastoma multiforme is intricately linked to this cancer's exceptional invasive capacity. We show here that SAHA limits the invasive capacity of a variety of glioma cell lines in vitro in both 2D and 3D assays. In 2D, our results indicate that SAHA has significant independent effects on proliferation, migration, and invasion. For C6 cells in 3D spheroid culture, we find that SAHA is not as strongly anti-proliferative as on an uncoated Petri dish. However, the effect of SAHA on invasive cell density and speed for cells cultured in spheroid is significant. The decreased invasive capacity of SAHA treated cells was found to occur both in post- and pre-treated spheroids, indicating SAHA's anti-invasive activity was preserved even in reorganized environments more permissive of invasion. Findings of decreased invasive speed and invasive cell density after SAHA treatment were robust over a number of cell lines with different mutations and different invasive behavior, suggesting our finding is general to glioma cells. Specifically, U87 cells lack functional PTEN, a tumor suppression gene, but have wildtype p53, another tumor suppression gene mutated in many human glioblastomas [48–50]. The LN18 rat cell line has a mutation in p53 but not in PTEN [51]. The F98 rat cell line was chosen because it is a particularly aggressive rat glioma [52]. Additionally, it is useful for comparison with F98EGFRvIII cells, which have been transfected with a mutant human epidermal growth factor receptor (EGFR) gene found in ~50% of human gliomas. This mutant EGFR is associated with increased proliferation and decreased apoptosis [53–56].

Our finding that invasive cell density and speed is similarly affected in all cell lines tested, in spite of differences in genetic profile, suggests the anti-invasive effect of SAHA on gliomas may be general. The findings on these different cell lines also support our hypothesis that at least a portion of SAHA's efficacy in limiting invasion in 3D collagen gels is

due to increased cell–cell adhesion. In C6 cells, this hypothesis was supported by gross reduction in number of invasive cells, loose organization of the proliferative cells near the spheroid rim that might otherwise be invasive, failure of cells to invade reorganized matrices, and increased tightness of early aggregates formed in the presence of SAHA. Tests on the additional cell lines also support this hypothesis, in that it was found that cells with dispersed (C6, U87), ring-like (F98), and compact (F98EGFRvIII) invasive patterns in 1.0 mg/ml collagen I in the absence of SAHA all displayed compact invasion patterns upon treatment with 5.0 μ M SAHA. The dispersed, ring, and compact invasive patterns in collagen I gels have previously been shown to correlate with increasing cadherin expression and increasing surface tension of cell aggregates in glioma cell lines and fresh glioma cells [39]. We note two potentially surprising findings from the study of different cell lines in spheroid: first, LN18 cells show an invasive pattern not previously described for glioma cells, with very loose aggregates and rounded cells, perhaps indicative of both low cell–cell and low cell–collagen adhesivity. The response of LN18 spheroids to SAHA also differed from that of the other cell lines: while the invasive cell density did decrease, the remaining invasive cells were quite round and at a reasonable distance from the spheroid body, perhaps indicating an amoeboid rather than mesenchymal migratory phenotype through the collagen I gels [57]. Another unexpected result was that the F98EGFRvIII spheroids were clearly limited in invasive capacity relative to cell lines without that mutation. Despite the general correlation of EGFR mutations with increased malignancy, a similar decrease in invasive capacity was found for U87 cells with EGFR mutations relative to U87 with wild type EGFR in collagen I matrices previously; this finding may be related to the absence of EGFR amplification that generally accompanies EGFR mutations in gliomas in vivo [41].

Quantitative RT-PCR was performed to potentially further clarify the molecular basis of the anti-invasive effects of SAHA on glioma cells. As reported in Section 3.7, of the 21 proteases and protease inhibitors interrogated, only the gene predicted to correlate with MMP-15 was signifi-

cantly affected. MMP-15 can directly dissolve a number of ECM components, though it does not cleave collagens [58]. However, this membrane-anchored MMP is a known activator of MMP-2 [59]. Our zymography results, however, do not show any notable increase in MMP-2 activity with SAHA treatment after 24 h, though perhaps interrogation after longer times would show enhanced MMP-2 activity following up-regulation of MMP-15. In that case increase in invasion would be expected, as opposed to both our findings and those in mouse models [20–22]. Of the cadherins and cell-adhesion molecules tested, PECAM was most strongly up-regulated. The two other genes most substantially affected were integrin β_4 and ectonucleoside triphosphate diphosphohydrolase 1 (ENTPD1). It is not immediately clear whether up-regulation of β_4 integrins or ENTPD1 should inhibit invasion in either collagen I based in vitro assays or in vivo. β_4 integrins have not been implicated in glioma invasion, though it has been shown that $\alpha_6\beta_4$ integrins, important in laminin adhesion, are expressed at substantial levels in a rat model of glioma [60], though another study found reduced levels of β_4 integrins in glioblastoma vascular proliferations relative to normal endothelial cells [61]. Other laminin receptors, including the β_1 integrins, have been given much more attention in glioma research, and are particularly important in collagen I rich environments, since $\alpha_2\beta_1$ is the only integrin important in both collagen I traction generation and remodeling [62]. ENTPD1 is a member of the NTPDase family, which has been shown to be expressed at low levels in C6 cells compared to astrocytes [63]. A study in which ATP digestion was induced by apyrase in a rat glioma model showed significant decrease in tumor growth, thus suggesting that the increase in ENTPD1 seen here may be related to decrease in C6 proliferation and overall aggression seen both in our study and in SAHA studies in mouse models [20–22,63,64]. PECAM is the most obvious candidate of the three highly up-regulated genes to be responsible for the decreased invasion and increased cell adhesivity seen in the presence of SAHA treatment of glioma cell lines. PECAM mediates endothelial cell-endothelial cell adhesion and migration [65], and is a pro-angiogenic molecule that has been found to be expressed by gliomas with microvascular proliferation [66]. While PECAM is not known to mediate cell–cell adhesion in glioma cell lines or glioma cells in vivo, it may have similar effects to that of the cadherins in collagen I environments [39,67,68]. We note that it has also been shown that SAHA can up-regulate E-cadherin [69] and SAHA does do so in our study, though not at a statistically significant level (up-regulation: 8.64, $p = 0.07$), and this may contribute to the diminished invasivity seen in the presence of SAHA [68].

5. Conclusion

We find that SAHA has significant effects on the migration and invasive capacity of glioma cells in 2D and 3D in vitro assays. In 2D, we show that SAHA has significant independent effects on glioma cell proliferation, migration, and invasion. In spheroid culture, SAHA limits both C6 glioma reorganization of collagen surroundings and invasion

into either isotropic or reorganized collagen environments. The decreased invasion in all glioma cell lines investigated does not appear to be related to decreased production or activity of matrix-metalloproteases and is instead proposed to be related to increased cell–cell adhesion. This is supported by results of the adhesion assay on C6 cells, alteration of invasive patterns from dispersed and ring-like to compact in several cell lines, and up-regulation of genes potentially important in cell–cell adhesion.

Conflicts of Interest

None declared.

Acknowledgements

This work was supported by a Beckman Young Investigator Award to L.J.K. and an NSF ADVANCE Grant (SBE-0245014). We thank Prof. Paul Marks and Prof. Ronald Breslow for useful discussions. We thank Prof. Ronald Breslow and Dr. Jiaming Yang for providing SAHA and Prof. Peter Canoll for providing cells.

Appendix A. Supplementary material

Supplementary data associated with this article can be found, in the online version, at doi:10.1016/j.canlet.2009.12.006.

References

- [1] A. Giese, M. Westphal, Glioma invasion in the central nervous system, *Neurosurgery* 39 (1996) 235–250.
- [2] T.S. Surawicz, F. Davis, S. Freels, E.R. Laws, H.R. Menck, Brain tumor survival: results from the national cancer data base, *J. Neurooncol.* 40 (1998) 151–160.
- [3] F.G. Davis, S. Freels, J. Grutsch, S. Barlas, S. Brem, Survival rates in patients with primary malignant brain tumors stratified by patient age and tumor histological type: an analysis based on surveillance, epidemiology, and end results (SEER) data, 1973–1991, *J. Neurosurg.* 88 (1998) 1–10.
- [4] Central Brain Tumor Registry of the United States (CBTRUS), 2002–2003. Primary Brain Tumors in the United States Statistical Report, 1995–1999. CBTRUS: Chicago.
- [5] A. Giese, R. Bjerkvig, M.E. Berens, M. Westphal, Cost of migration: Invasion of malignant gliomas and implications for treatment, *J. Clin. Oncol.* 21 (2003) 1624–1636.
- [6] A.C. Bellail, S.B. Hunter, D.J. Brat, C. Tan, E.G. Van Meir, Microregional extracellular matrix heterogeneity in brain modulates glioma cell invasion, *Int. J. Biochem. Cell Biol.* 36 (2004) 1046–1069.
- [7] T. Demuth, M.E. Berens, Molecular mechanisms of glioma cell migration and invasion, *J. Neurooncol.* 70 (2004) 217–228.
- [8] J.N. Bruce. 2006. Glioblastoma Multiforme. <<http://www.emedicine.com/MED/topic2692.htm>>.
- [9] S.K. Chintala, J.C. Tonn, J.S. Rao, Matrix metalloproteinases and their biological function in human gliomas, *Int. J. Dev. Neurosci.* 17 (1999) 495–502.
- [10] A.T.J. Belien, P.A. Paganetti, M.E. Schwab, Membrane-type 1 matrix metalloprotease (MT1-MMP) enables invasive migration of glioma cells in central nervous system white matter, *J. Cell Biol.* 144 (1999) 373–384.
- [11] E.I. Deryugina, M.A. Bourdon, G.X. Luo, R.A. Reisfeld, A. Strongin, Matrix metalloproteinase-2 activation modulates glioma cell migration, *J. Cell Sci.* 110 (1997) 2473–2482.
- [12] P.O. Esteve, P. Tremblay, M. Houde, Y. St-Pierre, R. Mandeville, In vitro expression of MMP-2 and MMP-9 in glioma cells following exposure to inflammatory mediators, *Biochim. Biophys. Acta–Mol. Cell Res.* 1403 (1998) 85–96.

- [13] P.A. Forsyth, H. Wong, T.D. Laing, N.B. Rewcastle, D.G. Morris, H. Muzik, K.J. Leco, R.N. Johnston, P.M.A. Brasher, G. Sutherland, D.R. Edwards, Gelatinase-A (MMP-2) gelatinase-B (MMP-9) and membrane type matrix metalloproteinase-1 (MT1-MMP) are involved in different aspects of the pathophysiology of malignant gliomas, *Br. J. Cancer* 79 (1999) 1828–1835.
- [14] M. Nakada, D. Kita, K. Futami, Y. Yamashita, N. Fujimoto, H. Sato, Y. Okada, Roles of membrane type 1 matrix metalloproteinase and tissue inhibitor of metalloproteinases 2 in invasion and dissemination of human malignant glioma, *J. Neurosurg.* 94 (2001) 464–473.
- [15] R. Sawaya, Y. Go, A.P. Kyritsis, J. Uhm, M. Venkaiah, S. Mohanam, Z.L. Gokaslan, J.S. Rao, Elevated levels of M-r 92,000 type IV collagenase during tumor growth in vivo, *Biochem. Biophys. Res. Commun.* 251 (1998) 632–636.
- [16] R.K. Nuttall, C.J. Pennington, J. Taplin, A. Wheal, V.W. Yong, P.A. Forsyth, D.R. Edwards, Elevated membrane-type matrix metalloproteinases in gliomas revealed by profiling proteases and inhibitors in human cancer cells, *Mol. Cancer Res.* 1 (2003) 333–345.
- [17] L.M. Coussens, B. Fingleton, L.M. Matrisian, Cancer therapy – matrix metalloproteinase inhibitors and cancer: trials and tribulations, *Science* 295 (2002) 2387–2392.
- [18] P.A. Marks, R. Breslow, Dimethyl sulfoxide to vorinostat: development of this histone deacetylase inhibitor as an anticancer drug, *Nat. Biotechnol.* 25 (2007) 84–90.
- [19] J.E. Bolden, M.J. Peart, R.W. Johnstone, Anticancer activities of histone deacetylase inhibitors, *Nat. Rev. Drug Disc.* 5 (2006) 769–784.
- [20] I.Y. Eyupoglu, E. Hahnen, R. Buslei, F.A. Siebzehnrubl, N.E. Savaskan, M. Luders, C. Trankle, W. Wick, M. Weller, R. Fahlbusch, I. Blumcke, Suberoylanilide hydroxamic acid (SAHA) has potent anti-glioma properties in vitro, ex vivo and in vivo, *J. Neurochem.* 93 (2005) 992–999.
- [21] H.C. Ugur, N. Ramakrishna, L. Bello, L.G. Menon, S.K. Kim, P.M. Black, R.S. Carroll, Continuous intracranial administration of suberoylanilide hydroxamic acid (SAHA) inhibits tumor growth in an orthotopic glioma model, *J. Neurooncol.* 83 (2007) 267–275.
- [22] D. Yin, J.M. Ong, J.W. Hu, J.C. Desmond, N. Kawamata, B.M. Konda, K.L. Black, H.P. Koeffler, Suberoylanilide hydroxamic acid, a histone deacetylase inhibitor: effects on gene expression and growth of glioma cells in vitro and in vivo, *Clin. Cancer Res.* 13 (2007) 1045–1052.
- [23] E. Galanis, K.A. Jaeckle, M.J. Maurer, J.M. Reid, M.M. Ames, J.S. Hardwick, J.F. Reilly, A. Loboda, M. Nebozhyn, V.R. Fantin, V.M. Richon, B. Scheithauer, C. Giannini, P.J. Flynn, D.F. Moore, J. Zwiebel, J.C. Buckner, Phase II trial of vorinostat in recurrent glioblastoma multiforme: a north central cancer treatment group study, *J. Clin. Oncol.* 27 (2009) 2052–2058.
- [24] E. Galanis, K. Jaeckle, J. Buckner, M. Maurer, J. Hardwick, V. Puduvalli, K. Lamborn, J. Kuhn, M. Prados, P. Wen, Vorinostat in glioblastoma multiforme (GBM): updated results from phase I and II trials provide the rationale for further clinical development, *Ann. Oncol.* 19 (2008) 249–250.
- [25] Y. Takada, A. Gillenwater, H. Ichikawa, B.B. Aggarwal, Suberoylanilide hydroxamic acid potentiates apoptosis, inhibits invasion, and abolishes osteoclastogenesis by suppressing nuclear factor-kappa B activation, *J. Biol. Chem.* 281 (2006) 5612–5622.
- [26] L.C. McGarry, J.N. Winnie, B.W. Ozanne, Invasion of v-Fos(FBR)-transformed cells is dependent upon histone deacetylase activity and suppression of histone deacetylase regulated genes, *Oncogene* 23 (2004) 5284–5292.
- [27] A.D.A. Tran, T.P. Marmo, A.A. Salam, S. Che, E. Finkelstein, R. Kabarriti, H.S. Xenias, R. Mazitschek, C. Hubbert, Y. Kawaguchi, M.P. Sheetz, T.P. Yao, J.C. Bulinski, HDAC6 deacetylation of tubulin modulates dynamics of cellular adhesions, *J. Cell Sci.* 120 (2007) 1469–1479.
- [28] L.T. Liu, H.C. Chang, L.C. Chiang, W.C. Hung, Histone deacetylase inhibitor up-regulates RECK to inhibit MMP-2 activation and cancer cell invasion, *Cancer Res.* 63 (2003) 3069–3072.
- [29] H.B. Liu, M.T. Voso, D. Gumiero, J. Duong, J.J. McKendrick, A.E. Dear, The anti-leukemic effect of a novel histone deacetylase inhibitor MCT-1 and 5-aza-cytidine involves augmentation of Nur77 and inhibition of MMP-9 expression, *Int. J. Oncol.* 34 (2009) 573–579.
- [30] M.S. Finnin, J.R. Donigan, A. Cohen, V.M. Richon, R.A. Rifkind, P.A. Marks, R. Breslow, N.P. Pavletich, Structures of a histone deacetylase homologue bound to the TSA and SAHA inhibitors, *Nature* 401 (1999) 188–193.
- [31] D.E. Levy, F. Lapiere, W.S. Liang, W.Q. Ye, C.W. Lange, X.Y. Li, D. Grobely, M. Casabonne, D. Tyrrell, K. Holme, A. Nadzan, R.E. Galaray, Matrix metalloproteinase inhibitors: a structure–activity study, *J. Med. Chem.* 41 (1998) 199–223.
- [32] H. Uchida, T. Maruyama, M. Ono, K. Ohta, T. Kajitani, H. Masuda, T. Nagashima, T. Arase, H. Asada, Y. Yoshimura, Histone deacetylase inhibitors stimulate cell migration in human endometrial adenocarcinoma cells through up-regulation of glycodefin, *Endocrinology* 148 (2007) 896–902.
- [33] K.T. Lin, S.H. Yeh, D.S. Chen, P.J. Chen, Y.S. Jou, Epigenetic activation of alpha 4, beta 2 and beta 6 integrins involved in cell migration in trichostatin A-treated Hep3B cells, *J. Biomed. Sci.* 12 (2005) 803–813.
- [34] A.J. Wilson, P.R. Gibson, Short-chain fatty acids promote the migration of colonic epithelial cells in vitro, *Gastroenterology* 113 (1997) 487–496.
- [35] K. Rombouts, T. Knittel, L. Machesky, F. Braet, A. Wielant, K. Hellemans, P. De Bleser, I. Gelman, G. Ramadori, A. Geerts, Actin filament formation, reorganization and migration are impaired in hepatic stellate cells under influence of trichostatin A, a histone deacetylase inhibitor, *J. Hepatol.* 37 (2002) 788–796.
- [36] M.J. Bissell, H.G. Hall, G. Parry, How does the extracellular-matrix direct gene-expression, *J. Theor. Biol.* 99 (1982) 31–68.
- [37] W. Paulus, W. Roggendorf, D. Schuppan, Immunohistochemical investigation of collagen subtypes in human glioblastomas, *Virchows Arch. A-Pathol. Anat. Histopathol.* 413 (1988) 325–332.
- [38] G. Bellon, T. Caulet, Y. Cam, M. Pluot, G. Poulin, M. Pytlnska, M.H. Bernard, Immunohistochemical localization of the basement-membrane and extracellular-matrix of human gliomas and meningiomas, *Acta Neuropathol.* 66 (1985) 245–252.
- [39] B. Hegedus, F. Marga, K. Jakab, K.L. Sharpe-Timms, G. Forgacs, The interplay of cell–cell and cell–matrix interactions in the invasive properties of brain tumors, *Biophys. J.* 91 (2006) 2708–2716.
- [40] L.J. Kaufman, C.P. Brangwynne, K.E. Kasza, E. Filippidi, V.D. Gordon, T.S. Deisboeck, D.A. Weitz, Glioma expansion in collagen I matrices: analyzing collagen concentration-dependent growth and motility patterns, *Biophys. J.* 89 (2005) 635–650.
- [41] A.M. Stein, T. Demuth, D. Mobley, M. Berens, L.M. Sander, A mathematical model of glioblastoma tumor spheroid invasion in a three-dimensional in vitro experiment, *Biophys. J.* 92 (2007) 356–365.
- [42] H.D. Kim, T.W. Guo, A.P. Wu, A. Wells, F.B. Gertler, D.A. Lauffenburger, Epidermal growth factor-induced enhancement of glioblastoma cell migration in 3D arises from an intrinsic increase in speed but an extrinsic matrix- and proteolysis-dependent increase in persistence, *Mol. Biol. Cell* 19 (2008) 4249–4259.
- [43] T.A. Ulrich, A. Jain, K. Tanner, J.L. MacKay, S. Kumar, Probing cellular mechanobiology in three-dimensional culture with collagen-agarose matrices, *Biomaterials* (in press). <http://www.sciencedirect.com/science?_ob=MIimg&_imagekey=B6TWPB-4XR5W6P-1-11&_cdi=5558&_user=18704&_orig=search&_coverDate=11%2F18%2F2009&_sk=999999999&view=c&wchp=dGLbVlb-zSkzS&md5=47acb61ceddfc95c0814d1e71d3d311e8&ie=sdarticle.pdf>.
- [44] http://www.sabiosciences.com/rt_pcr_product/HTML/PARN-013A.html.
- [45] J.S. Ungerstedt, Y. Sowa, W.S. Xu, Y. Shao, M. Dokmanovic, G. Perez, L. Ngo, A. Holmgren, X. Jiang, P.A. Marks, Role of thioredoxin in the response of normal and transformed cells to histone deacetylase inhibitors, *Proc. Natl. Acad. Sci. USA* 102 (2005) 673–678.
- [46] A.M. Stein, M.O. Nowicki, T. Demuth, M.E. Berens, S.E. Lawler, E.A. Chiozza, L.M. Sander, Estimating the cell density and invasive radius of three-dimensional glioblastoma tumor spheroids grown in vitro, *Appl. Opt.* 46 (2007) 5110–5118.
- [47] C.M. Salisbury, B.F. Cravatt, Activity-based probes for proteomic profiling of histone deacetylase complexes, *Proc. Natl. Acad. Sci. USA* 104 (2007) 1171–1176.
- [48] R.H. Frankel, W. Bayona, M. Koslow, E.W. Newcomb, p53 mutations in human-malignant in human-malignant gliomas – comparison of loss of heterozygosity with mutations frequency, *Cancer Res.* 52 (1992) 1427–1433.
- [49] E.G. Vanmeir, T. Kikuchi, M. Tada, H. Li, A.C. Diserens, B.E. Wojcik, H.J.S. Huang, T. Friedmann, N. Dtriboet, W.K. Cavenee, Analysis of the p53 gene and its expression in human glioblastoma cells, *Cancer Res.* 54 (1994) 649–652.
- [50] M.J. Park, M.S. Kim, I.C. Park, H.S. Kang, H. Yoo, S.H. Park, C.H. Rhee, S.I. Hong, S.H. Lee, PTEN suppresses hyaluronic acid-induced matrix metalloproteinase-9 expression in U87MG glioblastoma cells through focal adhesion kinase dephosphorylation, *Cancer Res.* 62 (2002) 6318–6322.
- [51] W. Wick, S. Wagner, S. Kerkau, J. Dichgans, J.C. Tonn, M. Weller, BCL-2 promotes migration and invasiveness of human glioma cells, *FEBS Lett.* 440 (1998) 419–424.

- [52] R.F. Barth, Rat brain tumor models in experimental neuro-oncology: the 9L, C6, T9, F98, RG2 (D74), RT-2 and CNS-1 gliomas, *J. Neurooncol.* 36 (1998) 91–102.
- [53] D. Hills, G. Rowlinsonbusza, W.J. Gullick, Specific targeting of a mutant, activated EGF receptor found in glioblastoma using a monoclonal antibody, *Int. J. Cancer* 63 (1995) 537–543.
- [54] W.L. Yang, R.F. Barth, G. Wu, L.J. Ciesielski, R.A. Fenstermaker, B.A. Moffat, B.D. Ross, C.J. Wikstrand, Development of a syngeneic rat brain tumor model expressing EGFRvIII and its use for molecular targeting studies with monoclonal antibody L8A4, *Clin. Cancer Res.* 11 (2005) 341–350.
- [55] C.T. Kuan, C.J. Wikstrand, D.D. Bigner, EGF mutant receptor vIII as a molecular target in cancer therapy, *Endocr. Relat. Cancer* 8 (2001) 83–96.
- [56] J.S. Smith, I. Tachibana, S.M. Passe, B.K. Huntley, T.J. Borell, N. Iturria, J.R. O'Fallon, P.L. Schaefer, B.W. Scheithauer, C.D. James, J.C. Buckner, R.B. Jenkins, PTEN mutation, EGFR amplification, and outcome in patients with anaplastic astrocytoma and glioblastoma multiforme, *J. Natl. Cancer Inst.* 93 (2001) 1246–1256.
- [57] P. Friedl, K. Wolf, Tumour-cell invasion and migration: diversity and escape mechanisms, *Nat. Rev. Cancer* 3 (2003) 362–374.
- [58] M.P. d'Ortho, H. Will, S. Atkinson, G. Butler, A. Messent, J. Gavrilovic, B. Smith, R. Timpl, L. Zardi, G. Murphy, Membrane-type matrix metalloproteinases 1 and 2 exhibit broad-spectrum proteolytic capacities comparable to many matrix metalloproteinases, *Eur. J. Biochem.* 250 (1997) 751–757.
- [59] C.J. Morrison, G.S. Butler, H.F. Bigg, C.R. Roberts, P.D. Soloway, C.M. Overall, Cellular activation of MMP-2 (gelatinase A) by MT2-MMP occurs via a TIMP-2-independent pathway, *J. Biol. Chem.* 276 (2001) 47402–47410.
- [60] S.C. Previtali, A. Quattrini, C.L. Pardini, R. Nemni, M.L. Feltri, E. Boncinelli, N. Canal, L. Wrabetz, Laminin receptor alpha 6 beta 4 integrin is highly expressed in ENU-induced glioma in rat, *Glia* 26 (1999) 55–63.
- [61] W. Paulus, I. Baur, D. Schuppan, W. Roggendorf, Characterization of integrin receptors in normal and neoplastic human brain, *Am. J. Pathol.* 143 (1993) 154–163.
- [62] J.A. Schiro, B.M.C. Chan, W.T. Roswit, P.D. Kassner, A.P. Pentland, M.E. Hemler, A.Z. Eisen, T.S. Kupper, Integrin-alpha-2-beta-1 (Vla-2) mediates reorganization and contraction of collagen matrices by human-cells, *Cell* 67 (1991) 403–410.
- [63] F.B. Morrone, D.L. Oliveira, P. Gamermann, J. Stella, S. Wofchuk, M.R. Wink, L. Meurer, M.I.A. Edelweiss, G. Lenz, A.M.O. Battastini, In vivo glioblastoma growth is reduced by apyrase activity in a rat glioma model, *BMC Cancer* 6 (2006) 226.
- [64] F.B. Morrone, M.C. Jacques-Silva, A.P. Horn, A. Bernardi, G. Schwartsmann, R. Rodnight, G. Lenz, Extracellular nucleotides and nucleosides induce proliferation and increase nucleoside transport in human glioma cell lines, *J. Neurooncol.* 64 (2003) 211–218.
- [65] C.S. Kim, T. Wang, J.A. Madri, Platelet endothelial cell adhesion molecule-1 expression modulates endothelial cell migration in vitro, *Lab. Invest.* 78 (1998) 583–590.
- [66] F. Aroca, W. Renaud, C. Bartoli, C. Bouvier-Labit, D. Figarella-Branger, Expression of PECAM-1/CD31 isoforms in human brain gliomas, *J. Neurooncol.* 43 (1999) 19–25.
- [67] K. Asano, C.D. Duntsch, Q.H. Zhou, J.D. Weimar, D. Bordelon, J.H. Robertson, T. Pourmotabbed, Correlation of N-cadherin expression in high grade gliomas with tissue invasion, *J. Neurooncol.* 70 (2004) 3–15.
- [68] M. Xia, M. Hu, J. Wang, Y. Xu, X. Chen, Y. Ma, S. Lei, Identification of the role of Smad interaction protein 1 in glioma, *J. Neurooncol.* 2009, <<http://www.springerlink.com/content/2746042453624274/fulltext.pdf>>.
- [69] T. Kumagai, N. Wakimoto, D. Yin, S. Gery, N. Kawamata, N. Takai, N. Komatsu, A. Chumakov, Y. Imai, H.P. Koeffler, Histone deacetylase inhibitor, suberoylanilide hydroxamic acid (Vorinostat, SAHA) profoundly inhibits the growth of human pancreatic cancer cells, *Int. J. Cancer* 121 (2007) 656–665.